Focused Ultrasound enabled Delivery and Uptake of Glioblastoma-Targeting Nanoparticles in vivo

Applicant:

Daniel Coluccia, MD

Department of Neurosurgery, Kantonsspital Aarau, CH-5001 Aarau, Switzerland

Research Fellow, The Arthur and Sonia Labatt Brain Tumour Research Center
Toronto Discovery District, 686 Bay Street, Toronto, Ontario, Canada, M5G 0A4

MR Center, Children's University Hospital of Zurich, CH-8032 Zurich, Switzerland

Host Institute:

James T. Rutka, MD, PhD, FRCSC, FACS, FAAP

Neurosurgeon, Director and Principal Investigator, Professor and Chair, Division of Surgery

The Arthur and Sonia Labatt Brain Tumour Research Center

Toronto Discovery District, 686 Bay Street, Toronto, Ontario, Canada, M5G 0A4

Correspondence:

Dr. Daniel Coluccia
Department of Neurosurgery, Kantonsspital Aarau, CH-5001 Aarau, Switzerland

Research Fellow, Neuro-Oncology
The Arthur and Sonia Labatt Brain Tumour Research Center, Toronto, Ontario, Canada, M5G 0A4

Email: daniel.coluccia@gmail.com

1. Background and purpose

Brain Tumour: Of all cancers, brain tumours represent perhaps the most intimidating and difficult-to-treat type of tumour. Considering the estimated incidence of 60 per 100,000 population[2-4] for intracranial neoplasms including primary and metastatic lesions, the treatment of patients with brain tumours constitutes a significant obligation for health professionals and social institutions. In 2004, the annual cumulative costs for brain tumour care in Switzerland were estimated at a minimum of 175 million Swiss francs (only primary brain tumours, metastases not included), which – considering the prevalence – poses by far the highest per capita cost of all neurological diseases.[5] Glioblastoma (GBM) is the most common and aggressive primary brain tumour, resulting in disproportionately high rates of morbidity and mortality. With an annual incidence of up to 7 per 100,000, this malignant glioma reaches an annual age-adjusted mortality rate of approx. 4 per 100,000.[6] The median age at the time of diagnosis is 56-64 years, whereby 10% of patients are younger than 50.[7, 8] In contrast to other solid cancers, such as breast and colon tumours, no stage dependent cure can be expected; the disease is always fatal regardless of early detection and maximal therapy.[9] Despite their aggressiveness, the vast majority of malignant gliomas do not metastasize systemically. Compared to most cancers, where systemic disease control is often a major complicating issue, tumour control outside the central nervous system is usually not relevant for GBM.[9] This circumstance could provide reason to expect facilitated tumour control. However, a major factor determining therapeutic failure is the highly infiltrative characteristic of glioma cells. Undetectable by contemporary imaging diagnostics, they invade and migrate over considerable distances into normal and, from a functional point of view, often non-resectable brain parenchyma.[10] Contemporary standard treatment consists of maximal surgical resection, followed by concomitant radiotherapy and chemotherapy with temozolomide (TMZ).[9] With standard care, the median survival time after diagnosis is approximately 14.6 months.[7] GBM will inevitably recur after treatment whereby the median time to recurrence is estimated at 6.9 months.[7] The etiology of GBM is largely unknown. The only established environmental risk factor is exposure to elevated ionizing radiation.[11] Apart from some rare genetic tumour syndromes (Li Fraumeni, Turcot, Neurofibromatosis),[12] there is evidence supporting a possible role of cytomegalovirus infection in the transformation of glial cells into malignant glioma cells.[13] Ultimately, there is no recommendation for prophylactic procedures or lifestyle changes known to reduce the risk of GBM formation.[11]

Blood Brain Barrier: A major challenge affecting the development of drug therapies for brain cancer is the poor delivery of agents into the brain parenchyma. This hindrance results from the tightly regulated movement of ions, molecules and cells within the capillary bed of the brain parenchyma – a phenomenon commonly referred to as blood-brain barrier (BBB).[14] The combination of endothelial tight junctions, surrounding pericytes, the basal membrane and cellular foot processes of astrocytes (which sheathe the blood vessels), results in a selective and specifically regulated exchange of substances.[15] Small nonpolar lipophilic substances generally cross passively, whereas polar or water-based compounds usually require active transport mechanisms.[16, 17] This characteristic, found across species, physiologically protects the brain from exposure to endogenous and exogenous toxins, and might also partly contribute to the observation that malignant glioma cells very rarely cross organ boundaries.[18] Even though the "tumour-blood-barrier" might be impaired to a certain extent, adequate delivery rate of well-established cancer drugs into the tumour bed is often impaired, regardless if they are intended for primary brain tumours or metastases.[14] As a result, only a few selected chemotherapeutic agents are being currently administered for brain cancer.[19] In order to overcome this limitation, different strategies can be pursued. The most obvious option is to raise the dosage in order to increase the concentration gradient across the cell membrane, at the risk of causing usually intolerable systemic toxicity. Intraoperative administration of drugs within the resulting tumour bed also has not proven substantial benefits.[9] Lastly, potential solutions either demand structural adaptation of chemotherapeutic agents or disruption of the BBB to allow drug delivery to the brain. Given the difficulty of molecularly redesigning and modifying agents, the latter strategy of opening the BBB appears more favorable. Ideally, an increase in BBB permeability should be non-invasive, safe, focal and reversible. To date, BBB disruption has only been achieved in a generalized and unselective manner, using either invasive intra-arterial applied osmotic agents or receptor-mediated mechanisms,[20, 21] which expose the unshielded brain to systemic toxins and include side effects to the renal and circulatory system.

Focused Ultrasound and Nanoparticles: Acoustic energy of high-intensity ultrasound focused precisely on a targeted location is able to thermo-coagulate tissue noninvasively as well as induce various biochemical reactions.[21, 22] The first attempts to evaluate this physical phenomenon for clinical use in the 1940s were hindered by a lack of thermometric control and exact determination of the focal point, but today it is possible to combine the

delivery of the ultrasonic beam with magnetic resonance image guidance, allowing thermometric monitoring and accurate targeting. Magnetic Resonance guided Focused Ultrasound (MRgFUS) has been approved and is increasingly used to noninvasively treat patients with uterine fibroids and bone metastasis. Additional applications are currently being evaluated in a number of advanced clinical studies.[23] Due to its capacity for image guidance and precise delivery of ultrasonic energy, MRgFUS is especially interesting for the treatment of brain diseases, where the small area of functional anatomy, as well as limited intraoperative visual orientation often impairs safe access to lesions. The ability of FUS to noninvasively ablate tissue may present a challenge to, or under certain circumstances, also complement surgery. Moreover, in contrast to radiosurgery, FUS does not involve ionizing radiation so that it may potentially be applied repeatedly. In 2009, at the MR center of the Children's University Hospital of Zurich, Prof. Ernst Martin and Beat Werner conducted the world's first successful clinical study on noninvasive MRgFUS thermo-ablation in the brain, where 12 patients were successfully treated for chronic pain disorder.[24] In further clinical studies in 2011, the use of MRgFUS for functional neurosurgery was successful and highly encouraging in treating patients with essential tremor through noninvasive thermal ablation of thalamic targets.[25, 26] Noninvasive MRgFUS recently received CE marking for functional neurosurgery. The first attempts to treat brain tumours by ablative FUS were completed in Israel in 2002 in a Phase I/II study.[27] While the ability to devitalize tumour tissue through thermo-coagulation could be demonstrated, a bony window had to be established at that time through a small craniotomy in order to allow penetration of ultrasonic waves. Today's transducer technology and software refinements allow for sufficient noninvasive penetration of therapeutic FUS through intact skin and calvaria. Having arranged and organized the first clinical trial to assess the safety and feasibility of MRgFUS for noninvasive brain tumour treatment, in collaboration with the MR center of the Children's University Hospital in Zurich, the applicant is in charge of this first Phase I study being carried out by the Kantonsspital Aarau (KEK AG 2010/026, ZH 2010-0543/3)[28] to evaluate eligible brain tumour patients. So far we have been able to enrol two patients. The first patient was a 33-year-old man enrolled by the neurosurgical team of the Kantonsspital St. Gallen. We performed two noninvasive MR-FUS sessions, whereas assessment of thermometric data and technical issues with the cavitation detection instrument used led to an early discontinuation of the sessions. The second patient was a 63-year-old patient from California, USA, presenting with tumor recurrence in the left thalamic and subthalamic region with a five-year survival after the first surgery for a Glioblastoma. In March 4th this year, a total of 25 sonications could be applied, while 17 sonications reached ablative temperatures of over 55°C with a maximum of 65°C. The MRI scan showed a well-circumscribed ablation of tumor tissue within the sonicated area without increasing perifocal edema. (Figure 1) The neurological examination showed an improvement of the preexisting right arm paresis; the patient is now able to lift the arm above shoulder level. Thus, we could conduct the first successful noninvasive thermal ablation of a brain tumour using FUS.

Parallel to the ablative capacities of FUS when using high frequency beam, FUS at lower frequencies has notably been shown to be able of target noninvasive and reversible opening of the BBB without tissue injury, in a variety of animals including non-human primates.[29-31] The mechanical interaction between the ultrasonic wave and the capillary bed presumably causes a transient rearrangement of BBB tight junction proteins and may also stimulate active transport, creating a transient window for drug delivery.[32, 33] As previously mentioned, conventional invasive and nonfocal opening of the BBB by osmotic agents counteracts the physiologic purpose of protecting the brain from systemic toxic effect, which is why it is rarely used in the clinical setting. FUS has the advantage of local, reversible, and presumably more efficient disruption of the BBB, which has been shown to last for approximately 4-6 hours in rats (Figure 2A).[32, 34] This feature allows for revaluation of established chemotherapeutics with proven therapeutic efficacy, which are used infrequently today for brain cancer due to insufficient passage through the BBB or adverse toxicity at therapeutic levels.[35] It also permits the study of newer therapeutic cancer agents such as antibodies. In fact, the possibility of vaster use of antibody-agents, which usually have limited ability to cross the BBB,[36] enables an application beyond that of cancer. In a recent study using a transgenic mice model for Alzheimer disease, FUS-facilitated delivery of iv-administered anti-amyloid antibodies into the brain resulted in marked reduction of plaques, whereas no effect was shown when FUS was not applied.[37] Moreover, it has been shown that the specificity and avidity of antibodies can potentially be enhanced when presented on the surface of nanoparticles (1-100 nm in diameter).[38] In addition to the use as carriers and amplifiers of therapeutic agents, nanoparticles have the capacity for manifold loading with molecules, which enables the designing of particles that can be simultaneously used as diagnostic and therapeutic means. Gold nanoparticles (GNPs), which are bio-inert and nontoxic,[39-41] appear very promising due to their extraordinary multiplexed labeling properties.[42] GNPs have been applied to enhance local radiotherapeutic effects,[43] deliver chemotherapeutics as well as

antibodies for cancer-targeting and treatment,[44, 45] transmit agents for thermotherapy[46] and deliver small interfering RNA for gene regulation.[47] Moreover, GNPs are already being used in FDA approved clinical trials.[48, 49] While the transfer of GNPs through the BBB is a major obstacle, studies from the affiliated research group showed that by using transcranial (tc) MR-guided FUS, 50nm polyethylene glycol (PEG) coated GNPs could be selectively delivered across blood vessels into the brain parenchyma in the rat (Figure 2).[34] While these PEG GNPs where not additionally labeled, the next step was to show that GNPs could be tagged and used as a scaffold for diagnostic and therapeutic means. It was hypothesized that GNPs in conjugation with a Raman reporter molecule[50] could be delivered into the brain to facilitate imaging of GNPs and cells. Spectral detection of GNPs with surface enhanced Raman scattering (SERS) tags is a well accepted and evolving technique for highly specific molecular imaging of cancer cells in vitro and in vivo.[51, 52] Raman reporter molecules can be detected and distinguished to ultra high sensitivity and specificity by Raman spectroscopy, making the spectrum analogous to a fingerprint.[53] Implementation of this nanotechnology for malignant brain tumours is encouraging given that labeled particles have been shown to be internalized into the tumour mass, enabling detection of tumour margins during surgical resection.[54] In contrast to optical modalities using fluorescence detection, Raman spectroscopy does not show photo bleaching; it allows for acquisition of signal from tissue at greater depth from the imaging surface and can be combined with conventional immunohistochemistry or confocal fluorescence microscopy.[51, 53] In fact, Raman scattering resolving microscopes which can sharply differentiate brain tumours in vivo have already been produced[55], and small flexible endoscopic devices including fiber optic-based Raman spectroscopy have been used in a pilot clinical study in humans.[56] In a prior experiment performed by the affiliated research group, SERS capable GNPs were delivered noninvasively to the brain tumour margin in rats using tcMRgFUS. The results were confirmed using microscopy and Raman spectral imaging. The particles where shown to be widely distributed at the tumour front within the extravascular tumour tissue. The distribution of in vivo delivered SERS GNPs at cellular and subcellular level was not assessed. While the delivery of GNP at the tumour front is a promising result for pursuing the objective of targeted tumour therapy, tuning the nanoparticle specificity for GBM cells is a further challenge to extend or optimize directed therapy. Cell receptors may therefore be used as a target for nanoparticle homing to tumours, enhancing the delivery ratio. In a subanalysis, our research group[1] showed that SERS-capable GNPs loaded with monoclonal endothelial growth factor receptor (EGFR) antibody were avidly internalized by EGFR-expressing GBM cells in vitro, whereas internalization of GNPs without antibody loading was much lower and more random (Figure 3-6). In this context it must be noted that 40-60% of GBM cases exhibit EGFR amplification and EGFR overexpression.[57]

The purpose of this study is to show that tagged and EGFR-antibody loaded GNPs can also be delivered and internalized by GMB cells in vivo when using FUS and may facilitate concurrent diagnosis and therapy.

Hypothesis of the current study

- In an orthotopic tumour mouse model, GBM cells that express EGFR will take-up antibody functionalized SERS GNPs after parenchymal delivery by tcMRgFUS. In control groups (A, B, C) with unspecific labeled SERS GNPs (A), GBM cells with less EGFR expression (B), or without FUS (C) the distribution of SERS GNPs into the tumour tissue will be distinctly less (C) or showing lower rates of specific GBM cell internalization or colocalization with endosomes/multivesicular bodies (A, B). The uptake of SERS GNPs will mainly occur in the GBM cells relative to neurons and normal astrocytes.

- Functionalized SERS GNPs allow multiplexed in vivo visualization and tracking of GBM tumour cells in an orthotopic tumour mouse model using Raman spectroscopy. Internalization of SERS GNPs into GBM cells concedes complementary in vitro diagnostics using confocal-fluorescent microscopy, immunohistochemistry and Raman microscopy.

- SERS GNP carrying agents against various structures in GBM cells can be delivered through tcMRgFUS, allowing in vivo mapping of agents and cells. This will enable concurrent diagnosis and therapy and provide an additional plane in the visualization of anti-tumour effect in vivo, as well as in vitro.

Aim of the current study

The aim of the current study is to show that a significant uptake and specific delivery of EGFR targeted SERS GNPs into GBM cells is achievable using transcranial MRgFUS in vivo. The applicant will assess the steady-state plasma

concentration and elimination curve for SERS GNPs after intravenous injection and tcMRgFUS in macrophage depleted mice and determine whether there is a dose-dependent increase of SERS GNP signal in normal and tumour-infiltrated brain tissue. The extent and specificity of nanoparticle uptake by tumour cells in vivo and in vitro will be determined and the effect of timing and concentration on uptake will be recorded using Raman microscopy, immunohistochemistry, confocal-fluorescence microscopy and Transmission Electron Microscopy (TEM). Furthermore, we will determine the potential of distinguishing and tracking different GBM cells after loading with specific SERS GNPs in vitro and coinjecting them into the brain of mice. Once significant uptake and tracking of functionalized SERS GNPs is shown, we can move onto multiplexed labeling of tumour cells in vivo and introduce therapeutic agents for targeted tumour therapy.

2. Methods

Animal procedures have been approved by the Animal Care Committee of Sunnybrook Research Institute and in compliance with the guidelines established by the Canadian Council on Animal Care and the Animals for Research Act of Ontario. The applicant will perform all animal and in vitro experiments, interpretation and statistical analysis, as well as writing the manuscripts to be published. The host institution will supply all equipment and infrastructure. The experiments will be arranged in order to build on GNP:

i) Delivery
ii) Uptake and Tracking
iii) Therapeutic Conjugates

Experiment 1– Delivery, Uptake, Tracking: Silica coated GNPs (Cabot Security Materials, Massachusetts, USA) tagged with a Raman reporter for SERS are functionalized using thiol-reactive chemistry to covalently link the EGFR-Antibody (Panitumumab, Amgen Inc., CA, USA) and Cyto647 fluorophore to the silica surface (αEGFR-SERS440).[58] As a non-specific antibody or non-antibody control, SERS-GNPs are functionalized with human immunoglobulin G (IgG-SERS421) or Methyl-PEG_{12} (mPEG12-SERS420), respectively.[58] In order to obtain an orthotopic brain tumour model, nude female NOD/SCID mice are implanted with enhanced green fluorescent protein (eGFP)-transfected human gliomablastoma cells (U251 and T98G due to high EGFR expression[1, 59]) via a stereotactic implantation device into the striatum (right frontal lobe, 5 micrL suspension containing 5 x 10^5 cells). As a control, animals are implanted U251 cells previously transfected with specific siRNA to inhibit EGFR expression (tf-U251).[60] The epidermal growth factor receptor expression is confirmed by Western blot for each cell line prior to implantation. Brain MRI (3.0 T) imaging 8 days post tumour cell implantation is performed to document tumour growth. Anesthesia is performed with a mixture of oxygen 0.8 L/min and 2% vaporized isoflurane. Untreated and tumour-bearing mice (with and without macrophage depletion by liposomal chlodronate) are injected with functionalized GNPs through the single tail vein (concentrations from 2 to 8 x10^8 particles per g body weight). Blood samples using cardiac puncture are taken at 30min, 2h, 4h, 8h, and 24h (anaesthesia under isoflurane, euthanasia using physical method). Steady state plasma concentration and elimination curve of the nanoparticles is determined by ICP-MS (inductively coupled plasma mass spectrometry) or absorbance at 544 nm using a NanoDrop 1000 UV-Vis spectrophotometer. Nanoparticle size distribution is assessed by Nanoparticle Tracking Analysis. GNP content in brain, brain tumour, liver, spleen and kidney is assessed by plasma mass (ICP-MS) and Raman spectroscopy. H&E histology, immunohistochemistry (staining against eGFP) and silver-enhanced in-situ hybridization are used in order to assess dose-dependent uptake and distribution.

Focused ultrasound and GNP Delivery: Tumour-bearing mice (U251 and T98G, controls tf-U251) are anaesthetized with isoflurane. An angio-catheter is inserted into the tail vein and the mouse is secured in a supine position on the FUS system, which is placed inside a 7.0T MRI. Intravenous infusion of αEGFR-SERS440 (controls with IgG-SERS421 and mPEG12-SERS420) is performed as a bolus. At the determined time of peak plasma concentration, four points at the tumour periphery defined by MR guidance are sonicated using our established protocol.[1] Animals are observed for signs of neurological impairment, including involuntary limb movement, lethargy, weakness, dehydration and weight loss. The uptake of nanoparticles is quantified using Raman signal in vivo through the intact skin and skull [54] or alternatively through a cranial window over the right frontal lobe.[61] The mice are sacrificed at varying time points following sonication and samples from freshly isolated brain, including

the interface between the tumour and surrounding brain tissue, are fixed in 3.7% formaldehyde and examined using high-resolution Raman microscopy (near-infrared 638 nm or 785 nm excitation laser, Renishaw). Results are correlated with fluorescent microscopy, H&E staining and silver enhancement histology to evaluate the distribution of GNPs between intracellular vs. extravascular and tumour-cells vs. astrocytes and neurons. In order to determine if αEGFR-SERS440 particles are taken up by cells through the same pathway as EGFR trafficking, confocal fluorescence microscopy is used to look for colocalization of the Cyto647 fluorescence signal with that of immunolabeled CD63, a protein marker for late endosomes/multivesicular bodies.[1, 62] The applicant expects that a time dependent movement of αEGFR-SERS440 into GBM U251 as well as T98G cells will be observed, whereas animals without FUS or controls (tf-U251 cells, IgG-SERS421, mPEG12-SERS420) will show less specific GNP uptake and cell internalization. Transmission electron microscopy will be used to further determine subcellular localization and particle density. Comparison of GNP distribution between groups is assessed by student's t-test with a P-value of 0.05 as significant. A minimum of ten 20x fields are photographed under fluorescence microscopy in order to count each cell showing at least 1 intracellular GNP, and the number of extracellular GNPs in the field. Once the applicant shows a substantial and specific in vivo delivery and uptake of αEGFR-SERS440 by GBM cells, the next step is to validate the repeated disruption of the BBB through tcMRgFUS without causing apparent morbidity to the animals, and to perform multiplexed labeling of GBM-cells. To this end, anti-EGFR antibody functionalized GNPs are tagged with three different SERS reporters (SERS 420, 421, 440). TcMRgFUS is performed on tumour bearing mice after tail vein injection of αEGFR-SERS420, 421, 440 at day 0, 3 and 6 in order to deliver the particles in tandem. Animals are observed for signs of neurological impairment and the uptake and distribution of the differently tagged nanoparticles is quantified and tracked using Raman signal in vivo. Mice are sacrificed at varying time points following sonication, and samples from freshly isolated brain are examined using high-resolution Raman microscopy, fluorescent microscopy and H&E staining in order to evaluate the intracellular and extravascular distribution of GNPs.

Experiment 2 – Tracking, Therapeutic conjugates: The next experimental study is aimed at presenting an orthotopic brain tumour model, which enables in vivo tracking and evaluation of targeted therapy for GBM tumours harbouring inhomogeneous cell populations. This model is designed to facilitate the study of targeted therapy against tumour proliferation (e.g. with the standard chemotherapeutic TMZ) and migration (e.g. with experimental siRNA). A brief background: Efficacy of alkylating chemotherapeutics like TMZ is limited at least in part by the DNA repair protein AGT encoded by the MGMT gene.[63] Unmethylated status of MGMT promoter is associated with higher MGMT protein expression, potentially resulting in TMZ resistance.[63] O^6-benzylguanine (BG) is an AGT substrate that irreversibly inactivates AGT and enhances the cytotoxicity of TMZ, both in vitro and in vivo.[64] First clinical studies combining BG with alkylating agents (BCNU, TMZ) were limited by the fact that enhanced cytotoxicity through systemic and untargeted BG counteracted at therapeutic levels as well the DNA repair protein in hematopoietic stem cells, thus provoking intolerable myelosupression.[64, 65] Targeted local therapy with GNP conjugated BG may therefore reduce toxicity. In terms of migration, the affiliated research group could show that by transfecting siRNA against the drebin encoding *human DBN1* gene (DBN1-siRNA), the high migration capacity of U87 cells was distinctly reduced, while the low-migration T98G cells showed only minor changes.[10]

U87-mCherry cells (known for drebrin-dependent high migration and low-adhesion to extracellular matrix[10], high EGFR expression[1] and methylated status of MGMT promoter showing high response to TMZ[66]) are incubated with αEGFR-SERS440 (~6000 GNP per cell) for 24 hours. Further, T98G cells (lower migration and higher adhesion with lower drebrin dependence,[10] high EGFR expression[59], unmethylated status of MGMT promoter[66] and higher resistance to TMZ[67]) are analogously incubated with αEGFR-SERS420 (Raman reporter dye with max. extinction at 420nm). Cellular uptake of the nanoparticles is confirmed using confocal fluorescence microscopy combined with Raman imaging (Cyto647 fluorescence signal for endosomes/multivesicular bodies, Phalloidin-Alexa 488 labeling for F-actin[1]) The incubated U87 and T98G cells are evenly mixed and injected into the right frontal lobe of NOD/SCID mice (mixU87-T98G) as described above. Potential release and exchange of GNPs within the mixed two cell groups is assessed in a subanalysis through fluorescence microscopy, combined with Raman imaging. The animals are anaesthetized 24h, 48h, 96h or 1-2 weeks after injection (or euthanized in a CO2 chamber to obtain brain slices), for in vivo visualization of SERS420 and SERS440 signal using transcranial Raman spectral microscopy or cranial window microscopy. This facilitates the mapping of migration and growth of the differently labeled GBM cells. Alternatively, in sacrificed animals the brain is washed in PBS, fixed with 3.7% formaldehyde and sectioned. A fixed starting point at the injection site is defined on whole-mount preparations of the brain and

the relative migration of one cell group versus the other is measured using ex vivo Raman imaging (Figure 7). Overlay of Raman spectral map on bright light microscopy of H&E stained sections allows for assessment of tumour cell morphology and their relationship to the surrounding tissue.[1] In addition, the change of the GNPs concentration per cell after growing and cell division as well as potential exchange of GNPs within the different cell types will possibly be evaluated.

These findings can be used to compare the effect on proliferation and migration (in vivo and in vitro) when BG and/or DBN1-siRNA are added in combination with TMZ. Depending on the successful conjugation of DBN1-siRNA and BG to silica coated SERS-reporter GNPs via thiol-gold bond[47, 68] (αEGFR-siRNA-SERS440, αEGFR-BG-SERS420, which will be synthetized and validated in collaboration with the Institute of Biomaterials and Biomedical Engineering, IBBME, University of Toronto), the applicant will set up a follow-up study and perform the in vitro and – depending on the results and time – in vivo delivery of these agents. For the in vitro studies, the U87 and T98G cells will be incubated with αEGFR-siRNA-SERS440 and/or αEGFR-BG-SERS420. The cell uptake of the tagged and functionalized GNPs will be assessed using confocal fluorescence microscopy combined with Raman imaging and TEM. The results will be compared with cells exposed to free DBN1-siRNA (HiPerfect QIAGEN, Toronto, Canada) or BG and GNP-drug-conjugates without EGFR-antibody. After whole cell lysis and fluorescence-assisted cell sorting of GNP loaded cells, cell incubation with a monoclonal anti-drebrin antibody for fluorescence microscopy and Western blot for drebrin expression will be used to assess the siRNA effect.[10] For cells additionally exposed to TMZ, AGT-protein expression is determined using immunohistochemistry, AGT activity is assessed using high-performance liquid chromatography, and methylation status of MGMT is evaluated with real time PCR. [69] Provided that an adequate cell uptake of αEGFR-siRNA-SERS440 and αEGFR-BG-SERS420 can be approved in vitro, the labeled cells will be used for the mixU87-T98G orthotopic model. After intraperitoneal (ip) administration of TMZ, the tumour cell proliferation and migration can thereafter be compared with the previous in vivo and in vitro results. Following tissue lysis and fluorescence-assisted cell sorting of GNP loaded cells, fluorescence microscopy, Western blot and PCR will be used to evaluate the effect on drebrin and AGT-protein. Depending on the results and the time remaining, the applicant will perform the in vivo delivery of αEGFR-siRNA-SERS440 and/or αEGFR-BG-SERS420 via tcMRgFUS after iv-injection in mixU87-T98G mice, in addition to ip-administration of TMZ. The abovementioned parameters for observing the tumour biology will then be reassessed.

3. Significance of the study

The results of this study will broaden the understanding of BBB disruption and drug delivery through FUS and enhance the development of antibody and small molecule agents against brain tumours. The additional capacities for optical tracking of these particles through Raman spectroscopy will extend the armamentarium for experimental drug testing and further investigations on the feasibility of clinical studies for targeted brain tumour therapy.

4. Outlook

Following the pioneering work in Zurich in 2009, Switzerland is perceived as a world leader in the clinical application of FUS for brain diseases. This reputation has been enforced recently by the world's firs successful noninvasive brain tumour ablation using MRgFUS. However, there is considerable mismatch with experimental research. This fact has been recognized, the purchase of a FUS device for animal studies has been approved and supported by Sinergia, and will be installed in April this year at the Animal Imaging Center of the ETH Hoenggerberg in Zurich. The first study investigating FUS enabled BBB opening and drug delivery in a rodent model is scheduled and will be conducted in Zurich by Prof. Leroux from the Institute of Drug Formulation and Delivery at the ETH, together with Prof. Weller from the Laboratory of Molecular Neuro-Oncology and Prof. Martin.[70] The presented research project in Toronto will give me the unique opportunity to significantly expand the knowhow about FUS for experimental, current and future clinical applications. There is increasing research activity in this exciting field. I will bring the know-how back to Switzerland and complement or extent the presented study in collaboration with the ETH and University of Zurich but also incorporate the acquired knowledge in future studies; making use of already existing collaborative partnerships and as well as extending the network.

5. Additional remarks

The applicant has no financial conflicts of interests to disclose in association with this application.

6. Figures

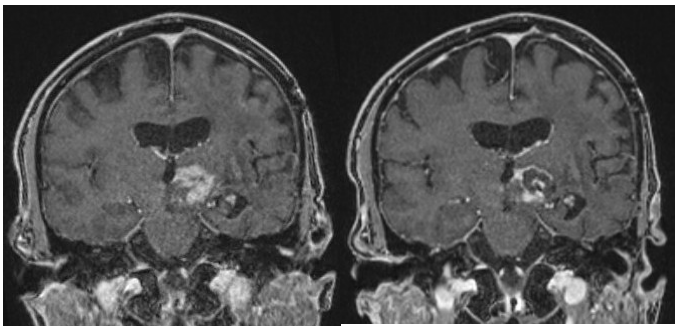

Figure 1. Pre-interventional (left) contrast-enhanced coronal MRI illustrating the enhancing tumor mass of a glioblastoma in the left thalamic and subthalamic region. Post-sonication (right) cornoal MRI shows a well-circumscribed partial resolution of enhancement, indicative for ablated tumor tissue. The patient was awake and responsive during the whole intervention.

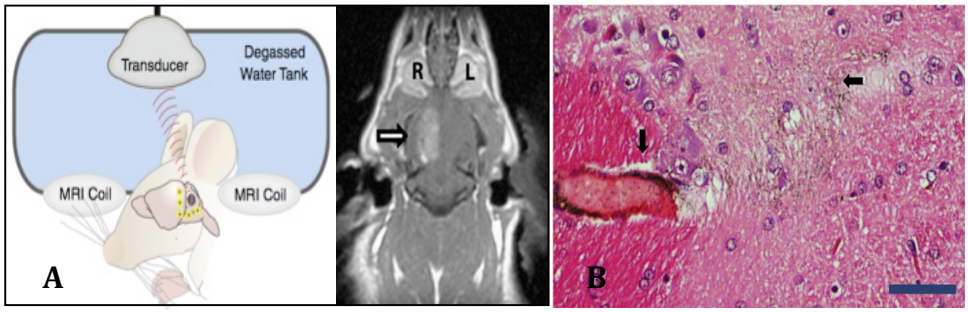

Figure 2. A: Animal is placed with part of the skull submerged in a water tank. Ultrasound transducer is placed and integrated in MRI-Scanner. FUS to the right hemisphere leads to a temporary disruption of the BBB as shown on axial MRI image, T1-weighted with gadolinium *(white arrow)*.

B: Silver enhancement and HE histology demonstrates *(black arrows)* perivascular and brain parenchyma localization of GNPs after tcMRgFUS. (Scale bar 50µm) (Etame et al.[34])

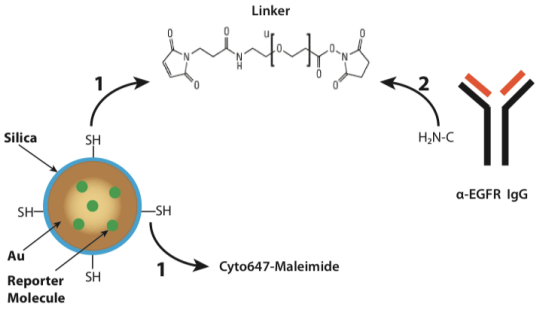

Figure 3. Synthesis of antibody functionalized silica shell gold nanoparticles. The succinimidyl-[(n-maleimid-propionamido)-octaethyleneglycol] ester and Cyto647-maleimide is conjugated to sulfhydryl groups on the silica shell under oxygen- free conditions (*arrow 1*). In the second step, the α-NH2-group of the N-terminus or the ε-NH2-group of lysine in the antibody reacts with the N-succinyl ester (*arrow 2*). The SERS Raman reporter molecule (*green ovals*) is shielded from the conjugation reactions within the silica shell and remains adsorbed to the gold core. (Diaz et al. [1])

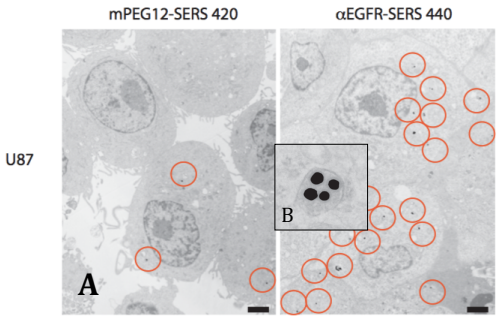

Figure 4. A: Transmission electron micrographs (TEM) images of U87 GBM cells at 5000x magnification, scale bar 2 µm. After 22 hours of incubation (ratio of 1000 GNPs: 1 cell and fixed GNP concentration at 0.66 fM) with unspecific SERS GNPs (mPEG12-SERS 420) or EGFR-antibody functionalized SERS GNPs (αEGFR-SERS440) U87 GBM cells show distinctive higher uptake of αEGFR-SERS440.

B: TEM images at 100,000x magnification showing αEGFR- SERS440 GNPs inside endosomes. (Diaz et al. [1])

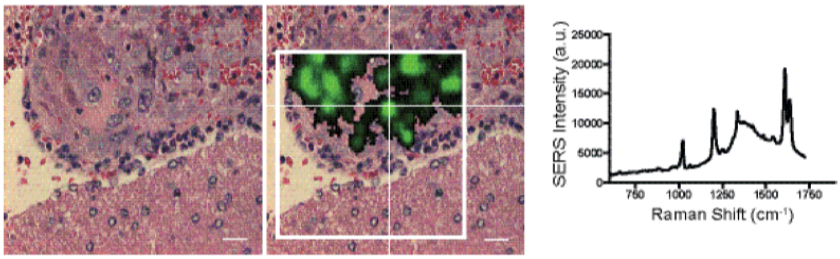

Figure 5. HE section of the interface between tumour and surrounding brain tissue with overlay of Raman spectral map on 40x bright light microscopy. U87 GBM cells were in vitro loaded with EGFR-Antibody labeled GNPs in conjugation with a Raman reporter molecule (αEGFR-SERS440 GNPs) and implanted into the frontal lobe of nude mice. GBM tumour cells can be defined additionally from surrounding gliosis and normal brain parenchyma using Raman spectrum and detection of specific spectrum from the SERS440 reporter molecule (*site defined by crosshairs*). Mapped region indicated by white box outline. Scale bars 20 µm. (Diaz et al.[1])

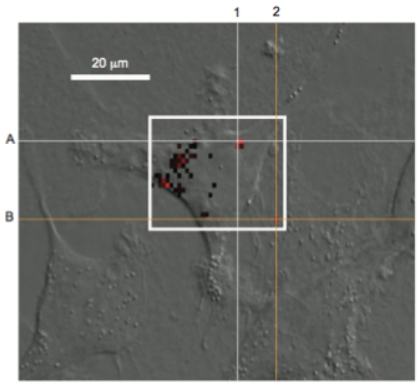

Figure 6. Raman confocal microscopy of αEGFR-SERS440 GNPs in A172 GBM cells. Raman spectra intensity map overlay on differential interference contrast images at 63x magnification showing intracellular GNPs after 24 hours of incubation. The white box outlines indicates the region of spectral mapping. At each pixel the intensity of red color represents the integrated photon counts for the spectral peak relative to the adjacent baseline. Position A1 and B2 show intracellular GNPs with Raman SERS 440 reporter while position B1 shows background silica fluorescence with no SERS 440 signal. (Diaz et al. [1])

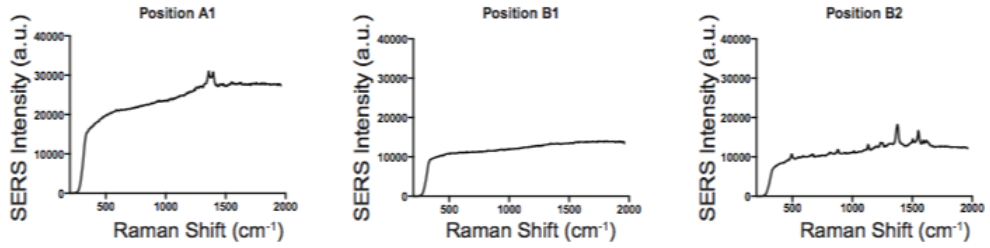

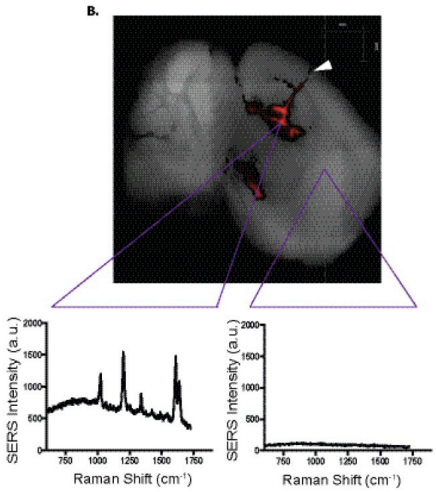

Figure 7. Ex-vivo whole mouse brain mount. Raman spectral map overlay (*red*) onto autofluorescence image generated by 470/50 nm excitation light with a 525/50 nm emission filter (*grey-scale*) showing dispersion of αEGFR-SERS440 loaded U87-mCherry cells after parenchymal injection. Needle entry site in the cortex indicated by the *white arrow*. Individual Raman spectra from regions positive and negative for αEGFR-SERS440 signal are depicted. (Diaz et al. [1])

7. References

1. Diaz RJ, McVeigh PZ, O'Reilly MA, et al. Focused ultrasound delivery of Raman nanoparticles across the blood-brain barrier: Potential for targeting experimental brain tumors. *Nanomedicine : nanotechnology, biology, and medicine* 2013.
2. Nayak L, Lee EQ, Wen PY. Epidemiology of brain metastases. *Current oncology reports* 2012; **14**(1): 48-54.
3. Ostrom QT, Gittleman H, Farah P, et al. CBTRUS statistical report: Primary brain and central nervous system tumors diagnosed in the United States in 2006-2010. *Neuro-oncology* 2013; **15 Suppl 2**: ii1-56.
4. DeAngelis LM. Brain tumors. *The New England journal of medicine* 2001; **344**(2): 114-23.
5. Andlin-Sobocki P, Jonsson B, Wittchen HU, Olesen J. Cost of disorders of the brain in Europe. *European journal of neurology : the official journal of the European Federation of Neurological Societies* 2005; **12 Suppl 1**: 1-27.
6. National Cancer Institute. http://www.cancer.gov/cancertopics/types/brain/ (accessed February 2014).
7. Stupp R, Mason WP, van den Bent MJ, et al. Radiotherapy plus concomitant and adjuvant temozolomide for glioblastoma. *The New England journal of medicine* 2005; **352**(10): 987-96.
8. Chakrabarti I, Cockburn M, Cozen W, Wang YP, Preston-Martin S. A population-based description of glioblastoma multiforme in Los Angeles County, 1974-1999. *Cancer* 2005; **104**(12): 2798-806.
9. Preusser M, de Ribaupierre S, Wohrer A, et al. Current concepts and management of glioblastoma. *Annals of neurology* 2011; **70**(1): 9-21.
10. Terakawa Y, Agnihotri S, Golbourn B, et al. The role of drebrin in glioma migration and invasion. *Experimental cell research* 2013; **319**(4): 517-28.
11. Ohgaki H, Kleihues P. Epidemiology and etiology of gliomas. *Acta neuropathologica* 2005; **109**(1): 93-108.
12. Louis DN, Ohgaki H, Wiestler OD, et al. The 2007 WHO classification of tumours of the central nervous system. *Acta neuropathologica* 2007; **114**(2): 97-109.
13. Soderberg-Naucler C, Rahbar A, Stragliotto G. Survival in patients with glioblastoma receiving valganciclovir. *The New England journal of medicine* 2013; **369**(10): 985-6.
14. Deeken JF, Loscher W. The blood-brain barrier and cancer: transporters, treatment, and Trojan horses. *Clinical cancer research : an official journal of the American Association for Cancer Research* 2007; **13**(6): 1663-74.
15. Daneman R. The blood-brain barrier in health and disease. *Annals of neurology* 2012; **72**(5): 648-72.
16. Pardridge WM. Blood-brain barrier drug targeting: the future of brain drug development. *Molecular interventions* 2003; **3**(2): 90-105, 51.
17. Loscher W, Potschka H. Drug resistance in brain diseases and the role of drug efflux transporters. *Nature reviews Neuroscience* 2005; **6**(8): 591-602.
18. Bernstein JJ, Woodard CA. Glioblastoma cells do not intravasate into blood vessels. *Neurosurgery* 1995; **36**(1): 124-32; discussion 32.
19. Cancer Research UK. http://www.cancerresearchuk.org/cancer-help/type/brain-tumour/treatment/chemotherapy/chemotherapy-drugs-for-brain-tumours - brain (accessed February 2014).
20. Rapoport SI. Osmotic opening of the blood-brain barrier: principles, mechanism, and therapeutic applications. *Cellular and molecular neurobiology* 2000; **20**(2): 217-30.
21. Emerich DF, Dean RL, Osborn C, Bartus RT. The development of the bradykinin agonist labradimil as a means to increase the permeability of the blood-brain barrier: from concept to clinical evaluation. *Clinical pharmacokinetics* 2001; **40**(2): 105-23.
22. Jagannathan J, Sanghvi NT, Crum LA, et al. High-intensity focused ultrasound surgery of the brain: part 1--A historical perspective with modern applications. *Neurosurgery* 2009; **64**(2): 201-10; discussion 10-1.
23. Medel R, Monteith SJ, Elias WJ, et al. Magnetic resonance-guided focused ultrasound surgery: Part 2: A review of current and future applications. *Neurosurgery* 2012; **71**(4): 755-63.
24. Martin E, Jeanmonod D, Morel A, Zadicario E, Werner B. High-intensity focused ultrasound for noninvasive functional neurosurgery. *Annals of neurology* 2009; **66**(6): 858-61.
25. Elias WJ, Huss D, Voss T, et al. A pilot study of focused ultrasound thalamotomy for essential tremor. *The New England journal of medicine* 2013; **369**(7): 640-8.
26. Lipsman N, Schwartz ML, Huang Y, et al. MR-guided focused ultrasound thalamotomy for essential tremor: a proof-of-concept study. *Lancet neurology* 2013; **12**(5): 462-8.

27. Ram Z, Cohen ZR, Harnof S, et al. Magnetic resonance imaging-guided, high-intensity focused ultrasound for brain tumor therapy. *Neurosurgery* 2006; **59**(5): 949-55; discussion 55-6.
28. ClinicalTrials.gov. http://clinicaltrials.gov/ct2/results?term=NCT01698437&Search=Search (accessed February 2014).
29. Etame AB, Diaz RJ, Smith CA, Mainprize TG, Hynynen K, Rutka JT. Focused ultrasound disruption of the blood-brain barrier: a new frontier for therapeutic delivery in molecular neurooncology. *Neurosurgical focus* 2012; **32**(1): E3.
30. Hynynen K, McDannold N, Vykhodtseva N, Jolesz FA. Noninvasive MR imaging-guided focal opening of the blood-brain barrier in rabbits. *Radiology* 2001; **220**(3): 640-6.
31. Marquet F, Tung YS, Teichert T, Ferrera VP, Konofagou EE. Noninvasive, transient and selective blood-brain barrier opening in non-human primates in vivo. *PloS one* 2011; **6**(7): e22598.
32. Sheikov N, McDannold N, Sharma S, Hynynen K. Effect of focused ultrasound applied with an ultrasound contrast agent on the tight junctional integrity of the brain microvascular endothelium. *Ultrasound in medicine & biology* 2008; **34**(7): 1093-104.
33. Shang X, Wang P, Liu Y, Zhang Z, Xue Y. Mechanism of low-frequency ultrasound in opening blood-tumor barrier by tight junction. *Journal of molecular neuroscience : MN* 2011; **43**(3): 364-9.
34. Etame AB, Diaz RJ, O'Reilly MA, et al. Enhanced delivery of gold nanoparticles with therapeutic potential into the brain using MRI-guided focused ultrasound. *Nanomedicine : nanotechnology, biology, and medicine* 2012; **8**(7): 1133-42.
35. Doolittle ND, Anderson CP, Bleyer WA, et al. Importance of dose intensity in neuro-oncology clinical trials: summary report of the Sixth Annual Meeting of the Blood-Brain Barrier Disruption Consortium. *Neuro-oncology* 2001; **3**(1): 46-54.
36. Chacko AM, Li C, Pryma DA, Brem S, Coukos G, Muzykantov V. Targeted delivery of antibody-based therapeutic and imaging agents to CNS tumors: crossing the blood-brain barrier divide. *Expert opinion on drug delivery* 2013; **10**(7): 907-26.
37. Jordao JF, Ayala-Grosso CA, Markham K, et al. Antibodies targeted to the brain with image-guided focused ultrasound reduces amyloid-beta plaque load in the TgCRND8 mouse model of Alzheimer's disease. *PloS one* 2010; **5**(5): e10549.
38. Barua S, Yoo JW, Kolhar P, Wakankar A, Gokarn YR, Mitragotri S. Particle shape enhances specificity of antibody-displaying nanoparticles. *Proceedings of the National Academy of Sciences of the United States of America* 2013; **110**(9): 3270-5.
39. Connor EE, Mwamuka J, Gole A, Murphy CJ, Wyatt MD. Gold nanoparticles are taken up by human cells but do not cause acute cytotoxicity. *Small* 2005; **1**(3): 325-7.
40. Male KB, Lachance B, Hrapovic S, Sunahara G, Luong JH. Assessment of cytotoxicity of quantum dots and gold nanoparticles using cell-based impedance spectroscopy. *Analytical chemistry* 2008; **80**(14): 5487-93.
41. Glazer ES, Zhu C, Hamir AN, Borne A, Thompson CS, Curley SA. Biodistribution and acute toxicity of naked gold nanoparticles in a rabbit hepatic tumor model. *Nanotoxicology* 2011; **5**(4): 459-68.
42. Kim BY, Rutka JT, Chan WC. Nanomedicine. *The New England journal of medicine* 2010; **363**(25): 2434-43.
43. Joh DY, Sun L, Stangl M, et al. Selective targeting of brain tumors with gold nanoparticle-induced radiosensitization. *PloS one* 2013; **8**(4): e62425.
44. Patra CR, Bhattacharya R, Wang E, et al. Targeted delivery of gemcitabine to pancreatic adenocarcinoma using cetuximab as a targeting agent. *Cancer research* 2008; **68**(6): 1970-8.
45. Tomuleasa C, Soritau O, Orza A, et al. Gold nanoparticles conjugated with cisplatin/doxorubicin/capecitabine lower the chemoresistance of hepatocellular carcinoma-derived cancer cells. *Journal of gastrointestinal and liver diseases : JGLD* 2012; **21**(2): 187-96.
46. Day ES, Thompson PA, Zhang L, et al. Nanoshell-mediated photothermal therapy improves survival in a murine glioma model. *Journal of neuro-oncology* 2011; **104**(1): 55-63.
47. Giljohann DA, Seferos DS, Prigodich AE, Patel PC, Mirkin CA. Gene regulation with polyvalent siRNA-nanoparticle conjugates. *Journal of the American Chemical Society* 2009; **131**(6): 2072-3.
48. Davis ME, Zuckerman JE, Choi CH, et al. Evidence of RNAi in humans from systemically administered siRNA via targeted nanoparticles. *Nature* 2010; **464**(7291): 1067-70.
49. Peer D, Karp JM, Hong S, Farokhzad OC, Margalit R, Langer R. Nanocarriers as an emerging platform for cancer therapy. *Nature nanotechnology* 2007; **2**(12): 751-60.
50. Clark RJ. Rayleigh, Ramsay, Rutherford and Raman--their connections with, and contributions to, the discovery of the Raman effect. *The Analyst* 2013; **138**(3): 729-34.

51. Qian X, Peng XH, Ansari DO, et al. In vivo tumor targeting and spectroscopic detection with surface-enhanced Raman nanoparticle tags. *Nature biotechnology* 2008; **26**(1): 83-90.
52. Song J, Zhou J, Duan H. Self-assembled plasmonic vesicles of SERS-encoded amphiphilic gold nanoparticles for cancer cell targeting and traceable intracellular drug delivery. *Journal of the American Chemical Society* 2012; **134**(32): 13458-69.
53. Vendrell M, Maiti KK, Dhaliwal K, Chang YT. Surface-enhanced Raman scattering in cancer detection and imaging. *Trends in biotechnology* 2013; **31**(4): 249-57.
54. Kircher MF, de la Zerda A, Jokerst JV, et al. A brain tumor molecular imaging strategy using a new triple-modality MRI-photoacoustic-Raman nanoparticle. *Nature medicine* 2012; **18**(5): 829-34.
55. Ji M, Orringer DA, Freudiger CW, et al. Rapid, label-free detection of brain tumors with stimulated Raman scattering microscopy. *Science translational medicine* 2013; **5**(201): 201ra119.
56. Zavaleta CL, Garai E, Liu JT, et al. A Raman-based endoscopic strategy for multiplexed molecular imaging. *Proceedings of the National Academy of Sciences of the United States of America* 2013; **110**(25): E2288-97.
57. Ohgaki H, Dessen P, Jourde B, et al. Genetic pathways to glioblastoma: a population-based study. *Cancer research* 2004; **64**(19): 6892-9.
58. Jokerst JV, Miao Z, Zavaleta C, Cheng Z, Gambhir SS. Affibody-functionalized gold-silica nanoparticles for Raman molecular imaging of the epidermal growth factor receptor. *Small* 2011; **7**(5): 625-33.
59. Yin D, Ogawa S, Kawamata N, et al. miR-34a functions as a tumor suppressor modulating EGFR in glioblastoma multiforme. *Oncogene* 2013; **32**(9): 1155-63.
60. Kang CS, Zhang ZY, Jia ZF, et al. Suppression of EGFR expression by antisense or small interference RNA inhibits U251 glioma cell growth in vitro and in vivo. *Cancer gene therapy* 2006; **13**(5): 530-8.
61. Burrell K, Hill RP, Zadeh G. High-resolution in-vivo analysis of normal brain response to cranial irradiation. *PloS one* 2012; **7**(6): e38366.
62. Pols MS, Klumperman J. Trafficking and function of the tetraspanin CD63. *Experimental cell research* 2009; **315**(9): 1584-92.
63. Hegi ME, Diserens AC, Gorlia T, et al. MGMT gene silencing and benefit from temozolomide in glioblastoma. *The New England journal of medicine* 2005; **352**(10): 997-1003.
64. Quinn JA, Desjardins A, Weingart J, et al. Phase I trial of temozolomide plus O6-benzylguanine for patients with recurrent or progressive malignant glioma. *Journal of clinical oncology : official journal of the American Society of Clinical Oncology* 2005; **23**(28): 7178-87.
65. Quinn JA, Pluda J, Dolan ME, et al. Phase II trial of carmustine plus O(6)-benzylguanine for patients with nitrosourea-resistant recurrent or progressive malignant glioma. *Journal of clinical oncology : official journal of the American Society of Clinical Oncology* 2002; **20**(9): 2277-83.
66. Yoshino A, Ogino A, Yachi K, et al. Gene expression profiling predicts response to temozolomide in malignant gliomas. *International journal of oncology* 2010; **36**(6): 1367-77.
67. Alonso MM, Gomez-Manzano C, Bekele BN, Yung WK, Fueyo J. Adenovirus-based strategies overcome temozolomide resistance by silencing the O6-methylguanine-DNA methyltransferase promoter. *Cancer research* 2007; **67**(24): 11499-504.
68. Engin S, Trouillet V, Franz CM, Welle A, Bruns M, Wedlich D. Benzylguanine thiol self-assembled monolayers for the immobilization of SNAP-tag proteins on microcontact-printed surface structures. *Langmuir : the ACS journal of surfaces and colloids* 2010; **26**(9): 6097-101.
69. Maxwell JA, Johnson SP, Quinn JA, et al. Quantitative analysis of O6-alkylguanine-DNA alkyltransferase in malignant glioma. *Molecular cancer therapeutics* 2006; **5**(10): 2531-9.
70. Focused ultrasound-mediated delivery of encapsulated MGMT antagonists for the treatment of temozolomide-resistant glioblastoma. http://www.research-projects.uzh.ch/p18478.htm (accessed February 2014).